Journal of Biomechanics 98 (2020) 109427

Contents lists available at ScienceDirect

Journal of Biomechanics

journal homepage: www.elsevier.com/locate/jbiomech
www.JBiomech.com

Short communication

Ultrasound shear wave elastography for measuring intracompartmental pressure of compartment syndrome using a turkey hind limb model

Yoichi Toyoshima [a], Jeremy Webb [b], Adriana Gregory [b], Mostafa Fatemi [c], Azra Alizad [b], Chunfeng Zhao [a,*]

[a] Division of Orthopedic Research, Department of Orthopedic Surgery, Mayo Clinic, Rochester, MN 55905, USA
[b] Department of Radiology, Mayo Clinic College of Medicine and Science, Rochester, MN 55905, USA
[c] Department of Physiology and Biomedical Engineering, Mayo Clinic College of Medicine and Science, Rochester, MN 55905, USA

ARTICLE INFO

Article history:
Accepted 13 October 2019

Keywords:
Diagnosis
Compartment syndrome
Fasciotomy
Trauma
Ultrasound shear wave elastography

ABSTRACT

Diagnosis and treatment of acute compartment syndrome are quite challenging. It is well known that compartment pressure is an important factor for diagnosing fasciotomy. However, the current technology to measure the pressure using a needle-catheter is invasive and painful. Recently ultrasound elastography has been used to measure soft tissue elasticity based on shear wave propagation speed. Because the muscle's elasticity is affected by the pressure within the compartment, ultrasound elastography might be a possible tool for the compartment pressure evaluation. Ultrasound shear wave elastography and pressure were simultaneously measured using a clinical ultrasound system and clinically used catheter in a turkey anterior-lateral and anterior-deep compartment under elevated pressures of baseline, 10, 20, 30, 40, and 50 mmHg using vascular infusion technique. Shear wave propagation speed increased linearly in proportion to the increase in intra-compartmental pressure. Strong correlation was observed between measured pressure and mean shear wave speed in each compartment (anterior-lateral compartment, mean $R^2 = 0.929$, $P < 0.001$; anterior-deep compartment, mean $R^2 = 0.97$, $P < 0.001$). Compared with anterolateral compartment pressure, anterior-deep compartment pressure was the same at the baseline; however, it was significantly higher at intended anterolateral compartment pressures of 20 and 30 mmHg ($P = 0.008$, $P = 0.016$). By using ultrasound shear wave elastography, the compartment pressure can be accurately measured. This noninvasive technology can potentially help surgeons for the early detection, monitoring, and prognosis of intra-compartmental pressure.

1. Introduction

Acute compartment syndrome (ACS) increases the intra-compartmental pressure (ICP) because of tissue injury in a physically-confined compartment for patients suffering from extremity trauma, such as fractures or crush injuries (Rorabeck and Clarke, 1978).

For trauma surgeons, early diagnosis and treatment of ACS are quite challenging (Wall et al., 2010; Bhattacharyya and Vrahas, 2004). Clinical symptoms for ACS patients, including pain, paresthesia, and pain with passive movement, are generally similar. Prospective studies on compartment syndrome are useful for clinical findings (Ulmer, 2002); however, clinical symptoms vary between patients because of an individual's tolerance levels. Therefore, ICP measurements are important for diagnosing and helpful for decision-making regarding fasciotomy. For a standard diagnosis of ACS, the pressure is measured by inserting a needle into the muscle (Wilson et al., 1997; Leversedge et al., 2011). However, this method is invasive and painful, especially if the ICP needs to be frequently measured. Hence, a noninvasive and reliable alternative diagnostic tool is desired.

Ultrasound shear wave elastography (SWE) estimates the elastic modulus of tissues from shear wave speed (SWS) induced by the acoustic radiation force of a focused ultrasound beam (Athanasiou et al., 2010; Park et al., 2014). SWE can provide quantitative in vivo measurements for soft tissue elasticity or stiffness by measuring SWS, which is inherently related to the elastic modulus (Garra, 2007). The SWE examination is noninvasive, convenient, and applicable to various clinical scenarios in which other approaches would potentially be inadequate.

The purpose of this study was to test if SWE could be used as a noninvasive tool for the assessment of ICP variations and simultaneous measurement of the ICP value in two compartments using a turkey leg model in vitro. We hypothesized that there would be a

* Corresponding author.
E-mail address: Zhao.Chunfeng@mayo.edu (C. Zhao).

https://doi.org/10.1016/j.jbiomech.2019.109427
0021-9290/

significant correlation between increased ICP and SWS, which could be measured using SWE.

2. Materials and methods

2.1. Anatomy

A turkey has a thin and soft skin like human and has less excess fat in their compartments than the pig, which is a common animal model for the compartment syndrome-related research. The anterior compartment is the common compartment involved compartment syndrome in humans, which corresponds to the anterior-deep and anterior-lateral compartments of a turkey. During preliminary experiments, we injected colored saline into the anterior-deep compartment and confirmed that the liquid was trapped within the compartment, and only ICP was increased. With further dissection, we identified that similar to the anatomy of the four-compartment human lower leg, the turkeys hind limb compartment was completely divided into the medial, anterior-lateral, anterior-deep, posterior-deep, and posterior compartments (Fig. 1).

2.2. Creation of the compartment model

We created a compartment model in which ICP was simultaneously increased in all compartments by the vascular infusion technique using six turkey limbs (Bourbon Red Tom Turkeys, 12+ months) obtained from turkeys sacrificed from other Institutional Animal Care and Use Committee (IACUC)-approved studies. The turkey's lower limbs were stored at −30 °C and thawed at 4 °C just two days before testing. A balloon catheter (Advance® ATB PTA Dilation Catheter; Cook Medical, Indianapolis, IN, USA) was inserted into the femoral artery, and the balloon was inflated just before branching toward the sural and fibular arteries. The femoral vein was suture ligated, and the proximal femoral vein was bound with vinyl tape to inhibit venous return.

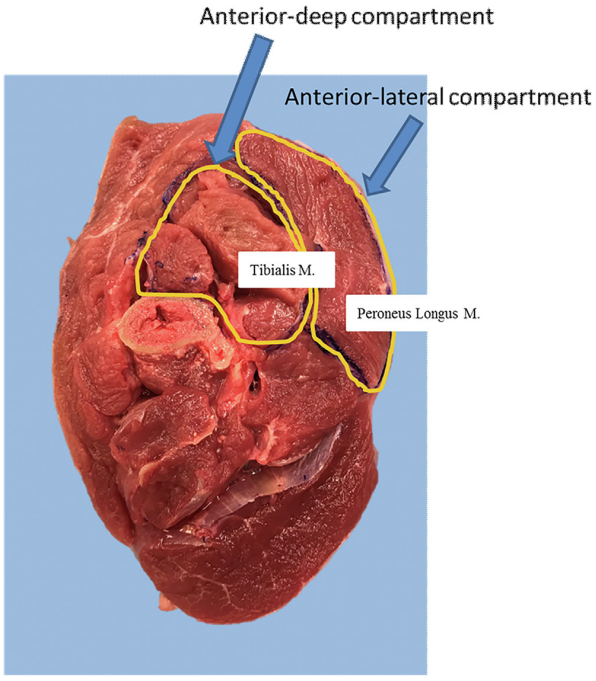

Fig. 1. Anatomy of the turkey hind limb. The anterior-deep compartment is composed of the flexor perforates digiti (FPD) and tibialis cranialis muscles, whereas the anterior-lateral compartment is composed of the peroneus longus muscle. The turkey hind limb compartment is completely divided into the medial, anterior-lateral, anterior-deep, posterior-deep and posterior compartments.

Subsequently, the saline solution was injected through the catheter. When the ICP of the anterior-lateral compartment reached the intended level, to maintain pressure, a Harvard pump (Catalog No: 881004, Harvard Apparatus, South Natick, MA, USA) was used. The ICP of the anterior-lateral compartment was increased stepwise beginning from the baseline, which was the prevalent pressure at the start of the experiment to 10, 20, 30, 40, and 50 mmHg, respectively. We set the range of ICP from 10 to 50 mmHg based on the common pressure range observed in a clinic within 12 h of acute compartment syndrome (McQueen and Court-Brown, 1996). The ICP of the anterior-deep compartment was then measured when the ICP of the anterior-lateral compartment reached the above values. Furthermore, we measured the ICP of the anterior-lateral and the anterior-deep compartment without moving either the specimen or the probe.

2.3. Measurement of intramuscular pressure

The induced ICP was monitored by a pressure measurement using a Pressure MAT Single-Use Sensor (PendoTECH, Princeton, NJ, USA) and recorded using the HART-Regen software (Harvard Apparatus). An 18-gauge needle connected to the piezoelectric microsensor was placed in the peroneus and tibialis cranialis muscle bellies. Furthermore, needle positioning was confirmed with ultrasound imaging.

2.4. SWE assessment

Using a commercial ultrasound system (GE LOGIQ E9; GE Healthcare, Milwaukee, WI, USA), SWE was assessed using a 9L-D linear array ultrasound transducer with musculoskeletal preset (GE Healthcare Japan, Tokyo, Japan). SWE measurements for each region were assessed independently in the plane parallel to the muscle fibers. The rectangular-shape elastography window covered the entirely anterior-lateral compartment and the anterior portion of the anterior-deep compartment during the ultrasound examination. The elastographic data were analyzed with a single circular region of interest (6 mm diameter) within the center of the rectangular area in each compartment (Fig. 2). The elasticity range was set from 0 to 180 kPa; 0–7.1 m/sec. For minimizing experimental variations caused by probe positioning or probe pressure, the elastography window was first allowed to stabilize for five seconds to obtain stable color-coded maps before the first elastography image was acquired. The second and third elastography images were then captured after three and six seconds (Koo et al., 2013). The two-dimensional SWE elastography method was used to create a color mapped elastogram. For minimizing tissue compression, an articulated arm was used to hold the ultrasound transducer in place. Assuming that tissues are homogeneous, the relationship is $E = 3\rho Vs^2$ (E = elastic modulus [kPa], ρ = muscle density which is assumed to be 1000 kg/m^3, Vs = shear wave propagation speed [m/s]) (Gennisson et al., 2005; Bercoff et al., 2004; Koo et al., 2014). A parameter related to tissue stiffness can be measured by measuring the propagation of SWS (Parker et al., 2011; Garra, 2007; Sigrist et al., 2017). The value obtained by dividing the measured SWS by the mean SWS at the baseline was used to determine the SWS ratio (rSWS).

2.5. Statistical analysis

The data following normal distribution were described as mean ± SD. The normal distributions of each data set were

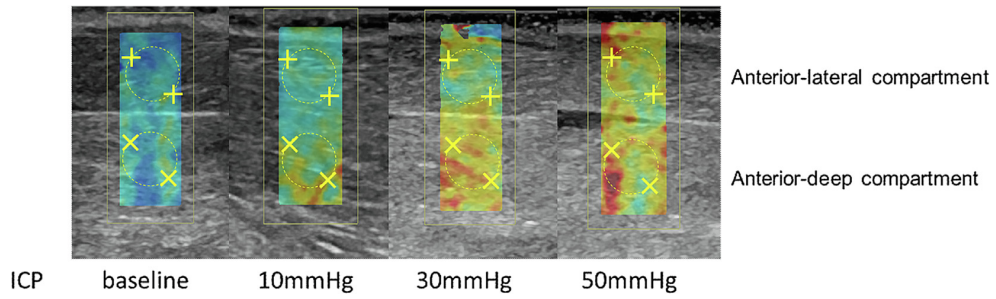

Fig. 2. Shear wave elastography (SWE) images showing the shear wave speed (SWS) at different intra-compartment pressures (ICPs).

evaluated by performing the Shapiro–Wilk test. For determining the relationship between measured ICP and SWS, Pearson's correlation was used. A linear equation was also computed by regression to further establish the relationship between measured ICP and SWS at different time points. A linear mixed-effects regression model assuming compound symmetry covariance structure was used to examine the effect of intended ICP and compartment group for measured ICP. The model for each intended ICP included compartment group as fixed effects and the specimen as a random effect. The multiplicity of comparisons was accounted by using Bonferroni correction. The statistical analyses were performed using SPSS ver. 22.0 (IBM Japan, Ltd., Tokyo, Japan). Statistical significance was set at $p < 0.05$.

3. Results

The typical SWE images in each ICP are shown in Fig. 2. The elasticity maps showed that the color distribution of the muscle was largely homogeneous. Fig. 3 shows the SWS findings of the anterior-lateral compartment and anterior-deep compartment at the measured ICPs. At baseline, the SWS was 2.45 (±0.11) in the anterior-lateral compartment and 2.19 (±0.24) in the anterior-deep compartment. In both compartments, there was an increase in the SWS with an increase in the ICP. Additionally, in both compartments, a strong correlation was observed between the mean measured ICP and the mean SWS (anterior-lateral compartment, mean $R^2 = 0.929$ (0.25), $P < 0.001$; anterior-deep compartment, mean $R^2 = 0.97$ (0.17), $P < 0.001$) (Fig. 4). The SWS increased sharply as the measured ICP increased from the baseline value to 10 mmHg and then, continued to increase gradually. The rSWS increased as the ICP increased in each compartment (Fig. 5).

The baseline ICPs for both compartments was the same; however, the ICP of the anterior-deep compartment was significantly higher than that of the anterior-lateral compartment within the lower ICP range (20 mmHg: $P = 0.008$, 30 mmHg: $P = 0.016$). Furthermore, when the intended ICP was 40 and 50 mmHg, there was no difference between the two compartments (Fig. 6).

4. Discussion

We created a compartment syndrome-like animal model using a vascular infusion technique in a turkey hind limb. We evaluated the relationship between the measured ICPs and SWS in superficial and deep compartments. We observed two important findings. First, SWS increased linearly with an increase in ICP. Second, ICP of the anterior-deep compartment was higher than that of the anterior-lateral compartment within the lower ICP range. To the best of our knowledge, this is the first study to evaluate the feasibility of SWE for ICP measurements in a compartment syndrome-like model.

Confirming muscle stiffness is an important clinical finding related to the risk of ACS. Compartment hardness is a direct expression of increased ICP and probably is the earliest objective indication of compartment syndrome (Steinberg, 2005; Sarvazyan et al., 2011; Olson and Rhorer, 2005). Recently, ultrasound technologies, including ultrasonic pulsed phase-locked loop (PPLL) and strain elastography, have been tested for ACS diagnosis. PPLL can detect very subtle fascia movement that corresponds to local arterial pulsation; thus, it could be useful for the assessment of ACS, especially at the early stage (Garabekyan et al., 2009; Lynch et al., 2004). However, PPLL needs to be further improved because many confounding factors affect fascia movement and many other conditions affect arterial pulsation (Shadgan et al., 2008). Strain

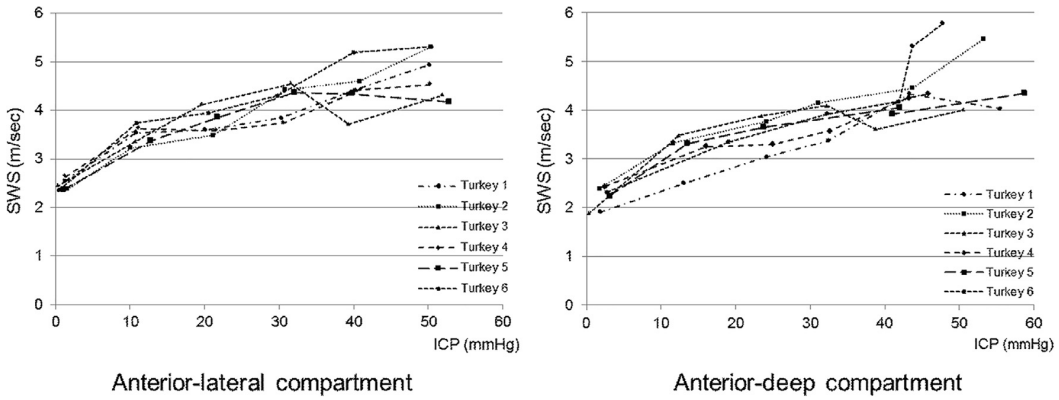

Fig. 3. The shear wave speed (SWS) of the anterior-lateral compartment and anterior-deep compartment at the measured intra-compartment pressure (ICP).

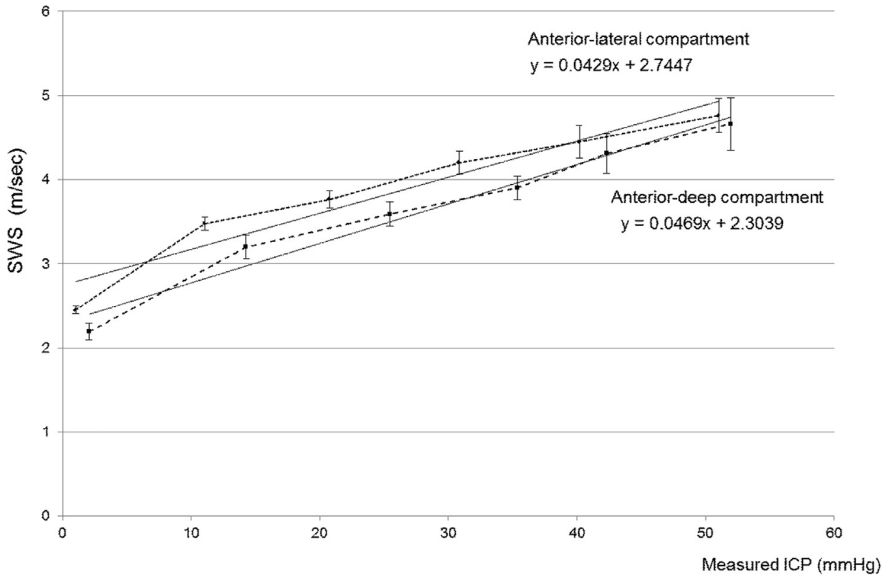

Fig. 4. The relationships between the shear wave speed (SWS) and intra-compartment pressure (ICP) in the anterior-lateral compartment and anterior-deep compartment (n = 6).

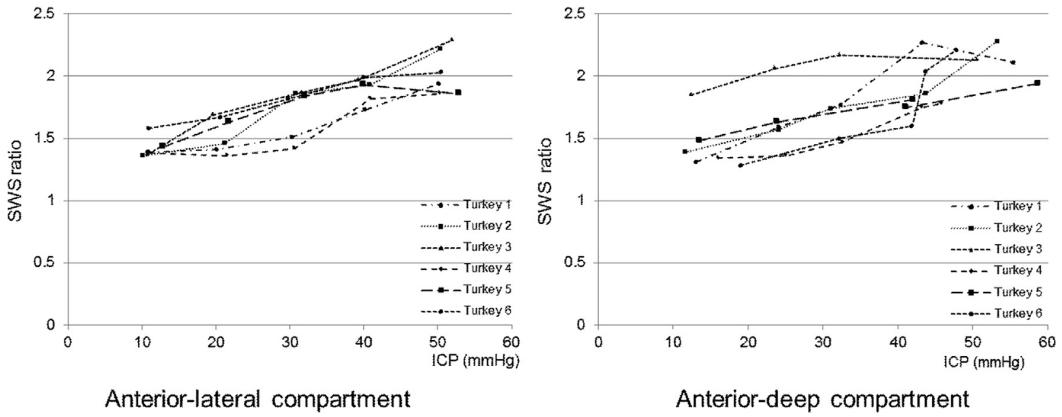

Fig. 5. The shear wave speed ratios of the anterior-lateral compartment and anterior-deep compartment at the measured intra-compartment pressure (ICP).

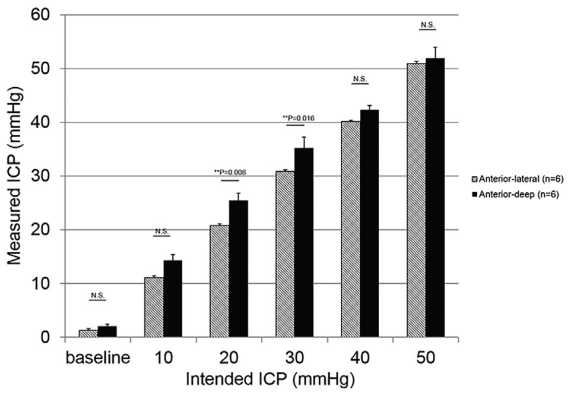

Fig. 6. The measured intra-compartment pressures (ICPs) in the anterior-lateral compartment and anterior-deep compartment when the intended ICPs of the anterior-lateral compartment were baseline value, 10, 20, 30, 40, and 50 mmHg.

elastography involves the use of an ultrasound probe to push the tissue, and ICP could be evaluated based on tissue deformation. This technology has some significant drawbacks because muscle strain is significantly affected by the tissues between the probe and muscle, including the skin and subcutaneous tissues, especially when the compartment is deep (Bloch et al., 2018; Itoh et al., 2006; Parker et al., 2011; Sellei et al., 2015; Nowicki and Dobruch-Sobczak, 2016). While strain elastography is a qualitative evaluation of tissue stiffness and can be less reliable owing to unknown distribution of pressure across tissue areas, SWE is a quantitative evaluation of tissue elastic properties (Prado-Costa et al., 2018; Paluch et al., 2016).

SWE is suitable for quantitatively evaluating mechanical properties such as muscle stiffness (Koo et al., 2014; Paluch et al., 2016; Winn et al., 2016). The SWS is not correlated with cross-sectional muscle area, physiological parameters (age, extremity lengths, body mass index, height, and weight), and sex at rest (Dubois et al., 2015; Koo et al., 2014; Souron et al., 2016). However, the SWS may be affected by increased muscle tone, muscle tissue

properties, muscle length, and mechanical muscle properties (Koo et al., 2014). We consider that evaluation using rSWS is useful for excluding the difference in individual variations. In actual clinical practice, it is often difficult to compare the affected and baseline condition. SWS of the tibialis anterior muscle in humans was found to be 2.1– to 3.2 m/s at rest, which was converted from Young's module or the shear elastic module, according to a formula described previously (Akiyama et al., 2016; Koo et al., 2014; Shinohara et al., 2010). SWS of the tibialis cranialis muscle in turkeys in this study was 2.45 (0.11) m/s, which is similar to the SWS findings in humans. We found a high correlation between increased ICP and increased SWS measurements using SWE, which is a useful tool to objectively quantify the elevated compartment pressure evaluated by physical findings, such as palpation.

An increase in soft tissue stiffness is associated with an increase in the internal pressure of soft tissue, owing to an increase in blood volume (Arokoski et al., 2005). The pathophysiology of ACS implicates a widely distributed change in the visco-elastic behavior of the muscle with edema (Sellei et al., 2015). Although previous ACS animal models were created by injecting saline directly or inserting a balloon into the compartment, we created a compartment syndrome-like model to inject saline into the femoral artery. ICP could be easily set and maintained according to the intended ICP. Furthermore, our animal model was able to demonstrate multiple ICP increases, which are simultaneously similar to ACS. In our study, SWS sharply increased with the increase in ICP from the baseline value to 10 mmHg and then, gradually increased. The sharp increase in SWS indicates that the saline-injected through the femoral artery enters each compartment, and the muscle volume and compartment pressure increase, causing the muscle to change from relaxation to tension. In our preliminary experiment (N = 3) using the same model, ICP increased to 50 mmHg and fasciotomy was performed, and then, ICP and SWS were measured. ICP was 7.6 (1.8) mmHg, and SWS was 2.39 (0.89) m/s at 5 min after fasciotomy. This result was consistent with the approximation formula obtained from the results of this study. It is unlikely that the water content in the muscle immediately decreased to the baseline value after the fasciotomy, and it is considered that the measured SWS was not affected by increased water content. We are planning further in vivo studies that will evaluate the relationship between ICP and SWS using SWE and histological evaluation to assess water content.

According to our results, when ICP of the superficial compartment is in 20 and 30 mmHg, the ICP of the deep compartment may have already exceeded 30 mmHg. It is believed that the fascia of the surficial compartment limits the expansion of the deep compartment. Therefore, when measuring ICP of the compartment, it is necessary to evaluate ICP is not only the superficial compartment but also the deep compartment (Matsen and Clawson, 1975; Heckman et al., 1994).

Our study has several limitations. The number of specimens in this study was small ($n = 6$); however, we were able to detect significant differences between various ICPs of two compartments. We used an 18-gauge needle as an actual clinical measurement tool of ICP. As reported by Bloch et al., the needle hole was occasionally occluded because of the muscle tissue; therefore, we frequently modified the needle position under ultrasonic guidance to properly measure the pressure for our study (Bloch et al., 2018; Whitesides et al., 1975). Whether the compartment pressure is controlled by our method in a live animal is unknown because a live animal has blood circulation and metabolism. Additionally, the responses of muscle fibers and intravascular connective tissues to increasing ICP in a live animal may be different from that in a dissected lower limb model. The relationship between the measured ICP and SWS identified in this study may not apply to humans because humans and turkeys have different muscle fiber types.

In conclusion, SWE can be recommended as a noninvasive method to detect an increase in ICP for cases of lower extremity compartment syndrome. Note that SWS increased significantly with an increase in ICP, making it possible to discriminate clinically significant differences for ICP levels.

Declaration of Competing Interest

There is no conflict of interest for all authors.

Acknowledgements

This study was supported by a grant from National Institutes of Health/National Institute of Arthritis and Musculoskeletal and Skin Diseases (AR067421).

References

Akiyama, K., Akagi, R., Hirayama, K., Hirose, N., Takahashi, H., Fukubayshi, T., 2016. Shear modulus of the lower leg muscles in patients with medial tibial stress syndrome. Ultrasound Med. Biol. 42, 1779–1783.
Arokoski, J.P., Surakka, J., Ojala, T., Kolari, P., Jurvelin, J.S., 2005. Feasibility of the use of a novel soft tissue stiffness meter. Physiol. Meas. 26, 215–228.
Athanasiou, A., Tardivon, A., Tanter, M., Sigal-Zafrani, B., Bercoff, J., Deffieux, T., Gennisson, J.L., Fink, M., Neuenschwander, S., 2010. Breast lesions: quantitative elastography with supersonic shear imaging–preliminary results. Radiology 256, 297–303.
Bercoff, J., Tanter, M., Fink, M., 2004. Supersonic shear imaging: a new technique for soft tissue elasticity mapping. IEEE Trans. Ultrason. Ferroelectr. Freq. Contr. 51, 396–409.
Bhattacharyya, T., Vrahas, M.S., 2004. The medical-legal aspects of compartment syndrome. J. Bone Joint Surg. Am. 86-a, 864–868.
Bloch, A., Tomaschett, C., Jakob, S.M., Schwinghammer, A., Schmid, T., 2018. Compression sonography for non-invasive measurement of lower leg compartment pressure in an animal model. Injury 49, 532–537.
Dubois, G., Kheireddine, W., Vergari, C., Bonneau, D., Thoreux, P., Rouch, P., Tanter, M., Gennisson, J.L., Skalli, W., 2015. Reliable protocol for shear wave elastography of lower limb muscles at rest and during passive stretching. Ultrasound Med. Biol. 41, 2284–2291.
Garabekyan, T., Murphey, G.C., Macias, B.R., Lynch, J.E., Hargens, A.R., 2009. New noninvasive ultrasound technique for monitoring perfusion pressure in a porcine model of acute compartment syndrome. J. Orthop. Trauma 23, 186–193. discussion 193-4.
Garra, B.S., 2007. Imaging and estimation of tissue elasticity by ultrasound. Ultrasound Q 23, 255–268.
Gennisson, J.L., Cornu, C., Catheline, S., Fink, M., Portero, P., 2005. Human muscle hardness assessment during incremental isometric contraction using transient elastography. J. Biomech. 38, 1543–1550.
Heckman, M.M., Whitesides, J.T., Grewe, S.R., Rooks, M.D., 1994. Compartment pressure in association with closed tibial fractures. The relationship between tissue pressure, compartment, and the distance from the site of the fracture. J. Bone Joint Surg. Am. 76, 1285–1292.
Itoh, A., Ueno, E., Tohno, E., Kamma, H., Takahashi, H., Shiina, T., Yamakawa, M., Matsumura, T., 2006. Breast disease: clinical application of US elastography for diagnosis. Radiology 239, 341–350.
Koo, T.K., Guo, J.Y., Cohen, J.H., Parker, K.J., 2013. Relationship between shear elastic modulus and passive muscle force: an ex-vivo study. J. Biomech. 46, 2053–2059.
Koo, T.K., Guo, J.Y., Cohen, J.H., Parker, K.J., 2014. Quantifying the passive stretching response of human tibialis anterior muscle using shear wave elastography. Clin. Biomech. (Bristol, Avon) 29, 33–39.
Leversedge, Fraser J., Moore, Thomas J., Peterson, Bret C., Seiler III, John G., 2011. Compartment syndrome of the upper extremity. J. Hand Surg. 36 (3), 544–559. https://doi.org/10.1016/j.jhsa:2010.12.008.
Lynch, J.E., Heyman, J.S., Hargens, A.R., 2004. Ultrasonic device for the noninvasive diagnosis of compartment syndrome. Physiol. Meas 25, N1–N9.
Matsen, F. A., 3RD & CLAWSON, D. K. 1975. The deep posterior compartmental syndrome of the leg. J Bone Joint Surg Am, 57, pp. 34–39.
McQueen, M.M., Court-Brown, C.M., 1996. Compartment monitoring in tibial fractures. The pressure threshold for decompression. J. Bone Joint Surg. Br. 78, 99–104.
Nowicki, A., Dobruch-Sobczak, K., 2016. Introduction to ultrasound elastography. J. Ultrason. 16, 113–124.
Olson, S.A., Rhorer, A.S., 2005. Orthopaedic trauma for the general orthopaedist: avoiding problems and pitfalls in treatment. Clin. Orthop. Relat. Res., 30–37
Paluch, L., Nawrocka-Laskus, E., Wieczorek, J., Mruk, B., Frel, M., Walecki, J., 2016. Use of ultrasound elastography in the assessment of the musculoskeletal system. Pol. J. Radiol. 81, 240–246.
Park, H.Y., Han, K.H., Yoon, J.H., Moon, H.J., Kim, M.J., Kim, E.K., 2014. Intra-observer reproducibility and diagnostic performance of breast shear-wave elastography in Asian women. Ultrasound Med. Biol. 40, 1058–1064.

Parker, K.J., Doyley, M.M., Rubens, D.J., 2011. Imaging the elastic properties of tissue: the 20 year perspective. Phys. Med. Biol. 56, R1–r29.
Prado-Costa, R., Rebelo, J., Monteiro-Barroso, J., Preto, A.S., 2018. Ultrasound elastography: compression elastography and shear-wave elastography in the assessment of tendon injury. Insights Imaging.
Rorabeck, C.H., Clarke, K.M., 1978. The pathophysiology of the anterior tibial compartment syndrome: an experimental investigation. J. Trauma 18, 299–304.
Sarvazyan, A., Hall, T.J., Urban, M.W., Fatemi, M., Aglyamov, S.R., Garra, B.S., 2011. An overview of elastography - an emerging branch of medical imagiNG. Curr. Med. Imag. Rev. 7, 255–282.
Sellei, R.M., Hingmann, S.J., Kobbe, P., Weber, C., Grice, J.E., Zimmerman, F., Jeromin, S., Hildebrand, F., Pape, H.C., 2015. Compartment elasticity measured by pressure-related ultrasound to determine patients "at risk" for compartment syndrome: an experimental in vitro study. Patient Saf. Surg. 9, 4.
Shadgan, B., Menon, M., O'Brien, P.J., Reid, W.D., 2008. Diagnostic techniques in acute compartment syndrome of the leg. J. Orthop. Trauma 22, 581–587.
Shinohara, M., Sabra, K., Gennisson, J.L., Fink, M., Tanter, M., 2010. Real-time visualization of muscle stiffness distribution with ultrasound shear wave imaging during muscle contraction. Muscle Nerve 42, 438–441.
Sigrist, R.M.S., Liau, J., Kaffas, A.E., Chammas, M.C., Willmann, J.K., 2017. Ultrasound elastography: review of techniques and clinical applications. Theranostics 7, 1303–1329.
Souron, R., Bordat, F., Farabet, A., Belli, A., Feasson, L., Nordez, A., Lapole, T., 2016. Sex differences in active tibialis anterior stiffness evaluated using supersonic shear imaging. J. Biomech. 49, 3534–3537.
Steinberg, B.D., 2005. Evaluation of limb compartments with increased interstitial pressure. An improved noninvasive method for determining quantitative hardness. J. Biomech. 38, 1629–1635.
Ulmer, T., 2002. The clinical diagnosis of compartment syndrome of the lower leg: are clinical findings predictive of the disorder?. J. Orthop. Trauma 16, 572–577.
Wall, C.J., Lynch, J., Harris, I.A., Richardson, M.D., Brand, C., Lowe, A.J., Sugrue, M., 2010. Clinical practice guidelines for the management of acute limb compartment syndrome following trauma. ANZ J. Surg. 80, 151–156.
Whitesides, T.E., Haney, T.C., Morimoto, K., Harada, H., 1975. Tissue pressure measurements as a determinant for the need of fasciotomy. Clin. Orthop. Relat. Res., 43–51
Wilson, S.C., Vrahas, M.S., Berson, L., Paul, E.M., 1997. A simple method to measure compartment pressures using an intravenous catheter. Orthopedics 20, 403–406.
Winn, N., Lalam, R., Cassar-Pullicino, V., 2016. Sonoelastography in the musculoskeletal system: current role and future directions. World J. Radiol. 8, 868–879.